Author Manuscript

Author Manuscript

Author Manuscript

Author Manuscript

HHS Public Access

Author manuscript

Chembiochem. Author manuscript; available in PMC 2022 February 02.

Published in final edited form as:

Chembiochem. 2021 February 02; 22(3): 585–591. doi:10.1002/cbic.202000645.

Covalent Linkage and Macrocylization Preserve and Enhance Synergistic Interactions in Catalytic Amyloids

Zsofia Lengyel-Zhand[a,†], **Liam R. Marshall**[a,†], **Maximilian Jung**[b], **Megha Jayachandran**[a], **Min-Chul Kim**[a], **Austin Kriews**[a], **Olga V. Makhlynets**[a], **H. Christopher Fry**[c], **Armin Geyer**[b], **Ivan V. Korendovych**[a]

[a] Department of Chemistry, Syracuse University, 111 College Place, Syracuse, NY 13244 USA.

[b] Department of Chemistry, Philipps-Universität Marburg, Hans-Meerwein-Straße 4, 35032 Marburg, Germany.

[c] Center for Nanoscale Materials, Argonne National Laboratory, Lemont, Illinois 60439 USA

Abstract

Self-assembly of short peptides into catalytic amyloid-like nanomaterials has proven to be a powerful tool in both understanding evolution of early proteins and identifying new catalysts for practically useful chemical reactions. Here we demonstrate that both parallel and antiparallel arrangements of β-sheets can accommodate metal ions in catalytically productive coordination environments. Moreover, synergistic relationships, identified in catalytic amyloid mixtures, can be captured in macrocyclic and sheet-loop-sheet species, that offer faster rates of assembly and provide more complex asymmetric arrangements of functional groups paving the way for future designs of amyloid-like catalytic proteins. Our findings show how initial catalytic activity in amyloid assemblies can be propagated and improved in more complex molecules, providing another link in a complex evolutionary chain between short, potentially abiotically produced, peptides and modern-day enzymes.

Graphical Abstract

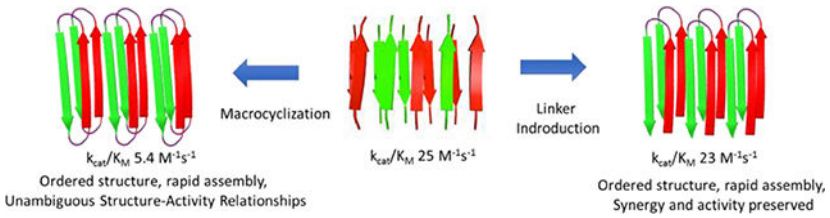

How might complexity arise from short peptides? Synergistic interaction so ubiquitous in catalytic amyloids can be propagated and enhanced by introduction of short peptide linkers. These results provide a crucial evolutionary link between catalytic assemblies of short peptides and modern day proteins.

ikorendo@syr.edu.

†These authors contributed equally to this work.

Supporting information for this article is given via a link at the end of the document.

Author Manuscript Author Manuscript Author Manuscript Author Manuscript

Keywords

self-assembly; catalysis; amyloids; synergistic interactions; peptides

Introduction

The mechanisms of emergence of enzymatic activity remain largely unclear. While most modern-day enzymes are at least 100 residues in length, spontaneous emergence of polypeptide chains of such a considerable length that would be functional is highly unlikely. This paradox led to a hypothesis that the earliest enzymes were markedly shorter and might have been formed from short peptides or polymers with repeating amino acid sequences that relied on self-assembly to achieve a folded structure.[1] Amino acids provide an excellent toolbox of functional groups for self-assembly and sequences as simple as dipeptides have been shown to form long, amyloid-like nanofibers.[2] Peptides as short as five residues can self-assemble into very stable fibrils, stabilized by both hydrogen bonding and hydrophobic packing.[3] This conformational diversity provides multiple opportunities for arrangement of catalytic groups.

Previously we have shown that *de novo* designed heptapeptides with alternating apolar and polar residues self-assemble into extended β-sheets stabilized through intermolecular association of the apolar residues in the sequence repeat.[4] These amyloids act as Zn^{2+}-dependent esterases, which rely on apolar residues to provide hydrophobic stabilization of the assembly, and His and other polar residues, located on the polar face of the strand, to ligate Zn^{2+} (Fig. 1).[5] Zn^{2+} helps stabilize the fibril formation, while also acting as a cofactor to catalyze hydrolysis of p-nitrophenyl acetate (pNPA), a substrate commonly used to probe esterase activity. The catalytic efficiencies shown by the assemblies are among the highest reported for any artificial catalysts of pNPA, reaching the levels shown by some enzymes by weight in the same reaction.[6] The repertoire of the chemical reactions that can be catalyzed by self-assembling peptide catalysts is rapidly growing and now includes redox transformations, phosphoester hydrolysis, enantioselective hydrogenation and cyclopropanation, among others.[7]

Most importantly, we have observed substantial positive synergistic interactions when mixing peptides with different sequences (Fig. 1).[4, 8] This finding shows how combinatorial screening of multiple functional groups can be done in a single fibril without the need for the covalent preparation of all possible amino acid combinations, which is fundamentally impossible.

At the same time some key questions posed by our previous work remain unanswered. Can short peptides be covalently linked to create more complex sequences with an activity gain, or at least without an activity loss? While the notion that modern day enzymes originated from covalent stitching of short fragments, a practical demonstration of how catalytic amyloid assemblies can evolve into more complex, asymmetric functional species remained elusive. And will the productive combinations of functional groups identified in mixing studies retain their beneficial interactions in more complex assemblies? Despite the explosion of the studies that look at mixed catalytic assemblies in the past decade to our

Author Manuscript Author Manuscript Author Manuscript Author Manuscript

knowledge there are no functional studies that demonstrate how peptide mix and, more specifically, if the activity improvement comes from stochastic arrangement of individual strands in the assembly they in fact mix stochastically at the molecular level.[2c]

From the evolutionary standpoint, β-sheets are uniquely well-suited for self-propagation.[9] Furthermore, multiple β-sheet subunits can be easily linked with β-turns with just a few additional residues (or potentially just one, if resorting to non-proteinogenic amino acids).[10] In addition to propagating functional information, the covalent linkers help stabilize and control assembly.[11] Various linkers were developed to mimic both parallel and antiparallel strand arrangement, allowing investigation of the elements favoring sheet-assembly. Moreover, macrocycles can be created by placing a linker at each end of the peptide, to allow for very rigid and unambiguous placement of functional groups relative to each other.

Results and Discussion

We have employed a variety of linkers to test various mechanistic aspects of catalytic amyloids (Scheme 1). We used ornithine for its simplicity and versatility, which allows for easy preparation of both β-hairpins and macrocycles,[12] and Hot=Tap, a synthetic bicyclic dipeptide which is a fusion of γ-hydroxythreonine and 4-thiaproline and offers a rigid, well-defined geometry that facilitates structural and functional studies.[13] Finally, we used two peptide loops (GGG and PSGSGSP, which we labelled as t^, as an ASCII-friendly depiction for Chinese/Japanese character for seven - 七) to create a less structurally restrained environment,[14] by extending the length of the peptide loop.

We focused on the leucine core peptides which, while still possessing relatively high activity in pNPA hydrolysis, assemble relatively slowly. This helps ensure proper equilibration of the system to achieve the thermodynamic minimum. Given the fact that all of the above mentioned linkers force the antiparallel arrangement of the strands, and we have previously observed parallel arrangements in the unconstrained assemblies,[5a] we ensured that the His residues are facing each other just like they would be in the parallel strand (Scheme 1).

All linker-containing peptides showed drastically improved rates of assembly relative to the parent heptameric peptides, even in the absence of metal ions (Figures S6,S7, Supporting Information). The results of the kinetic studies of the assemblies formed by different peptides are given in Table 1. The peptides that employed GGG, Hot=Tap, and ornithine as linkers all showed significantly lower activity than the parent fibril, despite forming β-sheet-rich assemblies as demonstrated by electron microscopy, circular dichroism studies, and NMR spectroscopy (Figures 2 and S2, S6, Supporting Information). Given the apparent difference in morphology between these fibrils and the ones formed by monomeric peptides, it is reasonable to assume that these linkers do not allow for assembly of the peptides in the productive conformations. The peptides with the t^ linker showed activity at the same levels as those observed for the parent fibril, suggesting that extra flexibility provided by a longer linker allows for productive assembly of the peptides. The morphology observed by TEM correlates with the ability of the linker to facilitate assembly of a catalytically productive amyloid. t^ linked peptides form long, thin fibrils (Figure 2D) quite distinct from the more amorphous aggregates seen with GGG, Hot=Tap and ornithine linkers (Figure 2a–c). This

Author Manuscript Author Manuscript Author Manuscript Author Manuscript

supports investigations which suggest it is the amyloid assembly which facilitates catalysis, separate from the ability of the individual peptide units to display β-sheet character.

Encouraged by this finding, we prepared peptides with glutamine substituted with arginine and tyrosine, residues previously shown to support catalysis in the 6 position. The catalytic efficiency shown by **t^RR** was equal to that of unconstrained peptide. Interestingly, for **t^YY** we observed a 3-fold loss in catalytic efficiency relative to the parent peptide, potentially suggesting substantial differences in atomic level structures for different catalytic amyloids, which can't be always adequately addressed with one size fit all linkers. Both prolines in the t^ linker are necessary for the productive arrangements of residues in the sheet-loop-sheet peptides, as their substitutions for glycine lead to substantially diminished catalytic activities despite preserved fibril formation (Figure S8, Supporting Information).

Having shown that short, catalytic amyloid-forming peptides can be covalently linked to form more complex species without activity loss, we investigated whether the synergy previously observed in fibril mixtures can be replicated in more complex, asymmetric peptides. First, we focused on the synergy between the two most active peptides Ac-LHLHLQL-NH_2 and Ac-LHLHLRL-NH_2. Excitingly, **t^QR** demonstrated an increase in activity relative to both **t^RR** and **t^QQ** as well as the parent peptides, demonstrating that the synergistic interactions between the peptides persist in a more constrained environment. The relative location of the residues in respect to the termini in the β-hairpin does not affect the catalytic efficiency, as both **t^QR** and **t^RQ** demonstrate identical values, although their k_{cat} and K_M parameters differ slightly. This finding validates our previously reported model that assumed random distribution of the strand without a preference for particular arrangements of strands.[4, 8]

Since the constrained nature of the sheet-loop-sheet in mixed composition peptides forces an alternating arrangement of strands containing different residues in the sixth position, analysis of their kinetic parameters offers mechanistic insight into the origins of the improved activity in the synergistic peptide mixtures. The observed increase in catalytic efficiency is driven exclusively by turnover frequency, as the Michaelis constants for **t^QR**, **t^RQ**, **t^RR**, and **t^QQ** are essentially the same. Next, we have tested whether previously identified synergy between arginine and tyrosine would still be present in the **t^**-linked peptides. Indeed, **t^YR** showed activity, which is substantially higher than that of **t^YY** and **t^ RR**, again demonstrating sustained synergistic interactions between the functional groups identified in the mixing studies. And just like in the case of **t^QR**, the observed increase in activity for **t^YR** is driven exclusively by the increase in turnover number (Table 1). This fact is quite surprising, given the relatively low K_M values for tyrosine containing catalytic amyloids. Taken together, these observations suggest that emergence of productive interactions between functional groups that directly improves efficient turnover is a more likely reason for higher catalytic activity, as opposed to an increase in bulk fibril hydrophobicity that would potentially lead to tighter substrate association. Importantly, the analysis presented above could not be devised by conducting similar studies on heptameric peptide mixtures (that necessarily will present several species stochastically distributed throughout the fibril) due to the requirement of introducing several approximation that may not be justified in the absence of detailed structural information.

Author Manuscript Author Manuscript Author Manuscript Author Manuscript

Given the flexibility of the linkers capable of productively joining catalytic amyloid-forming peptides, and the potential for alternative arrangements of fibrils as observed by Serpell and co-workers,[7a] we set out to confirm the observed synergistic effects in macrocyclic peptides that definitively lock the functional groups in place.

We employed ornithine as the linker of choice to create the macrocycles due to the synthetic simplicity, rigidity, well-established precedents for using it to create cyclic peptides,[12b] and the fact **oQQ** showed substantial (although diminished compared to **t^QQ**) activity in pNPA hydrolysis.

We have synthesized a series of macrocycles that contain two heptapeptide β-strands, connected by ornithines, to preserve the backbone of the parent fibrils while controlling the functional group placement as desired. We have also investigated the effect of the linkers, developed by Gellman and coworkers,[15] to provide a parallel arrangement of the strands (Scheme 2). First, we tested **mQQ$_a$**, a macrocycle that has Gln residues facing each other across the β-sheet, for its pNPA hydrolysis activity. While its catalytic efficiency of 6.3 ± 0.9 M^{-1} s^{-1} was lower than that of the unconstrained peptide assembly, it was nearly double the value of the corresponding β-hairpin, **oQQ**, suggesting that additional stabilization provided by the macrocyclic structure can help overcome the inefficiencies of the linker. The macrocycle that forces parallel arrangements of the two strands, **mQQ$_p$**, shows a value that is the same within the error of the measurement to that of **mQQ$_a$**, consistent with the notion that while both antiparallel and parallel arrangements of the stands are productive.[5b] The relative positioning of the residues is critical for the activity as the antiparallel peptide with the antiparallel arrangement of the strands **mQQ$_{a*}$** shows very little activity (Scheme 2, Table 2). These results are quite remarkable considering the difference in morphology between **mQQ$_a$** and **mQQ$_p$**, with the parallel macrocycles forming far more ordered and diffuse fibril networks upon self-assembly (Figure 3). Interestingly, the activity of peptides in this series seems to roughly correlate with the level of fibril dispersion linking the bulk morphology with catalytic activity, potentially suggestive of restricted access to the active site in some of the cases.

Based on these findings we utilized the ornithine linked antiparallel arrangement in subsequent studies due to the simplicity of its synthesis. Next, we sought to establish whether disruption of the internal hydrogen bonding in the macrocycles would affect their esterase activity. We incorporated single (R'=Me, R"=H, **mQQ$_m$**) and double (R'=R"=Me, **mQQ$_{mm}$**) N-methyl histidine residues to disrupt the intermolecular hydrogen bonding on one side of the macrocycle or both sides of the macrocycle, respectively. The methyl groups end up on the backbone amide groups facing away from the macrocyclic cavity (Scheme 2). Both **mQQ$_m$** and **mQQ$_{mm}$** had little to no activity and showed no aggregation in centrifugation studies (Figure S4, Supporting Information) demonstrating that even units with a sufficient number of ligating residues arranged in the correct order cannot produce catalytically efficient species. This observation is consistent with the requirement of forming extended aggregated self-assembled structures for productive catalysis in catalytic amyloids.

Having established the appropriate setting for testing the synergistic arrangements of heteromeric peptides, we synthesized macrocycles containing arginine and tyrosine in

Author Manuscript Author Manuscript Author Manuscript Author Manuscript

position 6 (Table 2). Consistent with the results observed for the glutamine containing peptides, we saw a uniform drop in activity in all macrocycles relative to the heptapeptide assemblies in all cases, irrespective of the parallel or antiparallel orientation of the strands. Importantly, the mixed arginine-tyrosine macrocycle (**mRY**) showed activity substantially higher than those of **mRR** and **mYY**, again demonstrating that the synergistic interactions previously identified in peptide mixtures persist in highly constrained environments.[4, 8] Relatively minor sequence changes can have quite significant impact on the morphology of the peptide assemblies. As demonstrated by AFM studies (Figure 3) macrocyclic peptides produced fibrillar structures with distinct morphologies in every single case. Despite such variability, all samples formed fibrils with heights varying between 1.2 to 2 nm, indicative of single cross-β bilayer with all zinc sites available for catalysis. Comparison of **mQQ$_p$** and **mQQ$_a$**, that represent the same parent sequence of LHLHLQL in the parallel and antiparallel arrangements, respectively, highlights this observation. While **mQQ$_p$**, assembles into long thin fibrils (Figure 3c), the assemblies formed by **mQQ$_a$** are thinner, with more globular aggregates observed within the micrograph (Figure 3a). The **mYR** assemblies display a morphology similar to that of **mQQ$_p$** whereas the micrographs of the dual tyrosine variant **mYY** show a fractal arrangement of peptides on the mica surface. The double tyrosine versions of both hairpin and macrocyclic catalytic amyloids have lower than expected hydrolytic activity, something not observed with the glutamine and arginine containing species. The observed correlation between the bulk morphology of the assemblies and catalytic activity is interesting, however, more in-depth structural characterization would be required to establish the detailed relationship between fibril composition, morphology, and catalytic activity.

While the results presented above demonstrate that synergistic interactions observed in peptide mixtures can be replicated within the constrained environments, it is not clear whether the new introduced constraints prevent further interstrand productive associations. In order to address this question, we have mixed **t^QQ** with **t^RR** and measured the catalytic activity of these mixtures (Table 1).

The peptide mixtures showed altered catalytic efficiencies compared to the individual peptides. Interestingly, the catalytic efficiency of a 1:1 mixture of **t^QQ** with **t^RR** is nearly identical to those of **t^QR** or **t^RQ**. As expected, mixing mirrored hairpins (**t^RQ** and **t^QR**) showed no synergy (Figure S25, Supporting Information). These observations demonstrate that the productive arrangements of functional groups, discovered in heptapeptide mixing experiments, are easily generalizable and applicable for more complex molecules in both intra- and intermolecular fashion.

Conclusion

In summary, we have reported that covalent attachment of short, catalytic amyloid-forming peptides stabilizes synergistic interactions that were identified during mixing of monomeric species. To our knowledge, this is the first practical demonstration of the ability of amyloids to retain and even enhance their catalytic properties upon introduction of covalent linkages. The catalytic activity of the resulting assemblies is highly dependent on the nature of the linker, favoring long, flexible linkers to properly accommodate the proper interstrand

Author Manuscript Author Manuscript Author Manuscript Author Manuscript

packing of the isolated peptides. We identified PSGSGSP, named t^, as a linker that does not perturb fibrilization and activity in catalytic amyloid-forming peptides. Identification of the linkers that are appropriate for the desired function, a highly non-trivial matter as demonstrated by Hecht and co-workers,[14, 16] will pave the way for future designs of amyloid-like catalytic proteins. Constraining the isolated strands together allowed us to determine that both parallel and antiparallel arrangements of β-strands can be productive in catalytic amyloids, making them versatile backbones for development of efficient nanomaterials for a variety of practical applications. By creating a constrained environment, we were able to demonstrate that even a two-strand arrangement with a sufficient number of ligating residues cannot provide the catalytically relevant species in the absence of self-assembly. Additionally, we have demonstrated that improved catalytic activities of peptide mixtures do indeed originate from productive interactions of different residues in a single fibril. This is an important observation in the context of the rapidly growing field of heteromeric peptide assemblies. Furthermore, productive arrangements or functional groups persist in more complex assemblies and the increased catalytic turnover found in the synergistic mixtures of peptides likely originates from higher turnover due to concerted action of multiple residues as opposed to faster fibrillation or more hydrophobic nature of the species. From the fundamental point of view, our finding shows that initial catalytic activity, found in catalytic amyloids assemblies, can be propagated and improved in more complex assemblies, providing another link in a complex evolutionary chain between short, potentially abiotically produced, peptides and modern-day enzymes.

Experimental Section

Peptide synthesis and purification.

The peptides were synthesized by manual fluorenylmethyloxycarbonyl (Fmoc) solid phase synthesis at elevated temperature using Rink Amide resin (Chem-Impex International). The resin was swelled in DMF then deprotected using 20% piperazine in DMF for 5 minutes. Each step consisted of i. Fmoc-deprotection with 20% piperazine in DMF for 5 minutes, ii. washing with DMF four times, iii. coupling of the amino acid in the presence of HCTU [2-(6-chloro-1H-benzotriazol-1-yl)-1,1,3,3-tetramethylaminium-hexafluorophosphate] and DIEA (N,N-diisopropylethylamine) (AA:HCTU:DIEA:resin 3:2.8:6:1), iv. washing with DMF twice. Each amino acid coupling step took 7 minutes. Cleavage of the peptides from resin and simultaneous side chain deprotection was achieved by treatment with a mixture of trifluoroacetic acid (TFA)/H_2O/triethylsilane (TES) (95:2.5:2.5, v/v) for 2 hours at room temperature. The crude peptides were precipitated and washed thrice with cold *tert*-Butyl methyl ether, then purified on a preparative reverse phase HPLC system (Varian ProStar 210) with C4 preparative column (Phenomenex), using a linear gradient of solvent A (0.1% TFA in water) and solvent B (90% CH_3CN, 10% H_2O, 0.1% TFA). The peptides were lyophilized, and their identities were confirmed by MALDI-TOF mass spectrometry (Bruker Autoflex III Smartbeam MALDI-TOF mass spectrometer). The purity of the peptides was evaluated on a Shimadzu Prominence UFLC instrument with an analytical Zorbax Eclipse XDB-C18 column (4.6 mm x 150 mm).

Author Manuscript Author Manuscript Author Manuscript Author Manuscript

Synthesis of htQQ.

The Hot=Tap turn mimetic was prepared according to the literature (Scheme S1).[1] The *N*-terminal carboxamide was established with the use of Rink-Amide-AM resin. The Rink-Amide-AM resin (68 mmol/g; 200–400 mesh; *Novabiochem*) was used as purchased. The protected amino acids were purchased from *IRIS Biotech*, *N,N'*-Diisopropylcarbodiimide (DIC, *TCI-Chemicals*) and Oxyma (*Novabiochem*) were used as coupling reagents. Peptides were synthesised on a microwave assisted peptide synthesiser (*Liberty Blue*, *CEM*). Fmoc-strategy was applied. The Rink-Amide-AM-resin (scheduled quantity: 0.1 mmol, 1.00 eq) ran through the following cycles of Fmoc-deprotection and amino acid coupling:

Fmoc-deprotection:

Cycle 1: T = 25 °C, $P_{microwave}$ = 0 W, t = 300 s, Cycle 2:T = 25 °C, $P_{microwave}$ = 0 W, t = 600 s with piperidine (20 w% in DMF, 3.00 mL/deprotection)

Amino acid coupling:

For amino acids except Fmoc-Arg(Pbf)-OH: T = 25 °C, $P_{microwave}$ = 0 W, t = 3600 s with Fmoc-protected amino acid (0.2 m in DMF, 5.00 eq, 2.5 mL/coupling), DIC (0.5 m in DMF, 5.00 eq, 1 mL/coupling) and Oxyma (1 m in DMF, 5.00 eq, 0.5 mL). For Fmoc-Arg(Pbf)-OH: T = 25 °C, $P_{microwave}$ = 0 W, t = 1500 s with Fmoc-protected amino acid (0.2 m in DMF, 5.00 eq, 2.5 mL/coupling), DIC (0.5 m in DMF, 5.00 eq, 1 mL/coupling) and Oxyma (1 m in DMF, 5.00 eq, 0.5 mL)

After the final Fmoc-deprotection the *N*-terminal acetylation was performed by treatment of the resin (equals 0.1 mmol peptide) with a solution of 0.5 mmol (5.0 equivalents) acetic anhydride and 0.2 mmol (2.0 equivalents) DIPEA in Dichloromethane (3.00 mL) for 1 h at room temperature. Afterwards the resin was washed with DMF, Methanol and DCM and dried under vacuum. Resin cleavage was performed with a mixture of TFA/H_2O/phenol/TIPS (88:5:5:2) for 5 h. Peptides were precipitated from cold diethyl ether (20 mL), washed two times with diethyl ether (20 mL), dried and lyophilised from water. Peptides were purified by semi-preparative reversed-phase HPLC on a Thermo Fisher Ultimate 3000 LC System with the following parameters: ACE 5 SuperC18, 150 mm x 10 mm, 15–40% B in 40 min (A: water + 0.1% TFA, B: acetonitrile + 0.085% TFA), 7.00 mL/min or Macherey Nagel Nucleodur C18 Gravity VP, 125 mm x 21 mm, 10–50% B in 30 min (Macherey Nagel Nucleodur C18 Gravity; A: water + 0.1% TFA, B: acetonitrile + 0.085% TFA), 15.0 mL/min. Analytical HPLC was performed with a *Thermo Fisher Ultimate 3000 LC System* under the following conditions. Column: ACE Ultracore 2.5 SuperC18, 150 mm x 2.1 mm. Gradient: 10–50% B in 10 min (A: water + 0.1% TFA, B: acetonitrile + 0.085% TFA). Flow rate: 0.45 mL/min

NMR-analytical Data of htQQ peptide.

The NMR measurements were performed with a BRUKER AVANCE II 600 (Figure S1, Figure S2 and Table S1). The peptide (2.0 mg) was dissolved in DMSO-d_6 (0.6 mL) and measured at temperatures from 300 K to 330 K. For the explicit assignment of the signals ^1H, ^{13}C, HSQC, TOCSY and NOESY-NMR-spectra were recorded and interpreted. The spectra were calibrated to the signal of DMSO-d_6 (2.50 ppm).

Author Manuscript Author Manuscript Author Manuscript Author Manuscript

Synthesis of antiparallel macrocycles.

i. Loading of the resin: 2-chlorotrityl chloride resin (84 mg, 1.2 mmol/g) was suspended and allowed to swell in dry CH_2Cl_2 for 30 min. The solvent was drained from the resin and a solution of Boc-Orn(Fmoc)-OH (0.1 mmol, 1 equiv.) in DIEA (6 eq.) and dry CH_2Cl_2 (4 mL) was added and the mixture was agitated for 1 hour at room temperature. The solution was then drained and the mixture of CH_2Cl_2/MeOH/DIPEA (17:2:1, 5 mL) was added. The mixture was gently agitated for 15 min, then the resin was washed with DMF (twice). *ii. Peptide coupling*: Procedure described above was followed for each peptide coupling steps. *iii. Cleavage of the peptide from the resin*: The linear peptide was agitated for 30 min with a solution of hexafluoroisopropanol (HFIP)/CH_2Cl_2 (1:4, 5 mL). The suspension was filtered, and the resin was washed with additional HFIP/CH_2Cl_2 (1:4, 5 ml), then with CH_2Cl_2 (2*10 mL). The combined filtrates were concentrated by rotary evaporation. *iv: Cyclization of the linear peptide*: The peptide was dissolved in 15 mL DMF and HOBt (68 mg, 0.5 mmol, 5 equiv.) and HBTU (200 mg, 0.5 mmol, 5 equiv.) were added to the solution. The mixture was stirred under nitrogen for 20 min, then DIEA (0.25 mL, 1.4 mmol, 14 equiv.) was slowly added to the solution. The mixture was stirred under nitrogen for 24 hours and then it was concentrated under reduced pressure. *v. Global deprotection and purification of the cyclic peptide*: The side chain deprotection was achieved by treatment with a mixture of trifluoroacetic acid (TFA)/H_2O/triethylsilane (TES) (95:2.5:2.5, v/v) for 2 hours at room temperature. The crude peptides were precipitated and washed with cold *tert*-Butyl methyl ether, then purified on a preparative reverse phase HPLC system with C4 preparative column, using a linear gradient of solvent A (0.1% TFA in Millipore solvent) and solvent B (90% CH_3CN, 10% H_2O, 0.1% TFA). The peptides were lyophilized, and their identities were confirmed by MALDI-TOF mass spectrometry. The purity of the peptides was evaluated on a UFLC instrument with an analytical XDB-C18 column.

Synthesis of N-to-N linker.

Succinic anhydride (1 g, 10.0 mmol) and 2-(trimethylsilyl)ethanol (0.625 g, 76 mL, 5.3 mmol) was dissolved in 20 mL toluene. Catalytic amount of 4-dimethylaminopyridine (DMAP) was added to the solution and the mixture was stirred at reflux for 10 hours. The solution was washed with 1 M HCl (3 × 50 mL) and NaCl solution (1 × 100 mL). The organic phase was dried over Na_2SO_4 and concentrated under reduced pressure to leave the final product as a clear oil (1.11 g, 96%).

Synthesis of parallel macrocycles.

Rink amide resin was suspended and allowed to swell in DMF for 30 min. Fmoc-Orn(alloc)-OH, the first seven amino acid residues and N-to-N linker (it was treated as an amino acid) were coupled using Fmoc-based solid synthesis described above. The allyloxycarbonyl protecting group was removed using $PdCl_2(PPh_3)_4$ (0.1 equiv.) and PPh_3 (1:3). $Me_2NH{\cdot}BH_3$ (40 equiv) was used as a scavenger. Next, the rest of the amino acids were coupled and then TMSE protecting group was removed using 1.0 M tetra-*n*-butylammonium fluoride (TBAF) in THF (3 eq, 0.9 mL). Macrocyclization was achieved on the resin, using standard coupling reagents (HCTU, DIPEA).The macrocycle was cleaved and purified using the method described above.

Author Manuscript Author Manuscript Author Manuscript Author Manuscript

Preparation of the peptide stocks and solutions.

The purified and lyophilized peptides were dissolved in 10 mM hydrochloric acid to make a 1.0 mM, pH 2 stock solution. The concentration of the stock solutions was determined on an Agilent 8453 UV-Vis spectrophotometer using absorbance at 214 nm. Extinction coefficient of the peptides were calculated using literature values.[2] The pH 8 stock solution of the peptides was prepared by mixing pH 2 peptide stock with buffer containing 25 mM Tris (pH 8) and 0.1 mM or 1 mM $ZnCl_2$. $ZnCl_2$ solution was prepared by dissolving Zn(II) salt in water to 50 mM concentration and this solution was further diluted to either 0.1 mM or 1 mM. The pH 2 stock solutions were stable for at least a week and the pH 8 solutions were prepared immediately before experiments.

Kinetic assay of *p*NPA hydrolysis.

Kinetic measurements were done at 25 °C on a BioTek Eon Microplate Reader using 96-well plates. *p*-nitrophenol acetate solutions in buffer (25 mM Tris, pH 8) were freshly prepared by dilution of a 0.1 M stock in acetonitrile to the final concentration of 195 μM, 375 μM, 570 μM and 750 μM. Substrate solutions of variable concentrations (150 μL) were added to Zn(II)-peptide pH 8 solution (60 μM for macrocycles and loop peptides other than t^, 100 μM for isolated peptides and t^ loops, 50 μL). Solutions of Zn(II) in buffer (1 mM $ZnCl_2$ in 25 mM Tris, pH 8, 50 μL) were used as a control for the background rate of reaction. The final acetonitrile content was 2% in all reaction mixtures. Once these components were mixed, absorbance of the product (p-nitrophenol) at 405 nm was monitored for five minutes. The initial linear portion of the kinetic trace was used to calculate V_0. Kinetic parameters were obtained by fitting the data to the Michaelis–Menten equation: $v_0 = k_{cat}[E]_0[S]_0/(K_M+[S]_0)$, where v_0 was calculated by dividing absorbance by extinction coefficient of the product (16,600 M^{-1} cm^{-1}).[3] For mixing experiments, stock solutions of peptides were prepared by dissolving lyophilized peptides in 10 mM HCl to the final concentration of 1 mM. Two stocks were mixed to produce 50 μL samples of peptides at various ratios (0, 8, 16, 24, 32, 40, 48, 55, 70, 85 and 100%). To each of these samples, 1.8 mL of 25 mM Tris (pH 8) containing 0.1 mM $ZnCl_2$ was added. 150 μL of the *p*NPA substrate solution was added to 50 μL of the final peptide mixture and hydrolytic activity was measured at three time points, at 0 hours and after 24 and 48 hours, as described above. Final concentrations in the reaction mixture were: 25 μM peptide, 195 μM substrate, 0.1 mM $ZnCl_2$ and 25 mM Tris (pH 8).

CD spectroscopy.

The CD spectra were collected on the Jasco J-715 CD spectrometer, using a step scan mode (4 sec averaging time) averaging three runs, using a quartz cuvette with a 0.1 cm path length. Samples were prepared as follows: 25 μL peptide stock (to the final concentration of 50 μM for macrocycles and 25 μM for peptides) and 275 μL buffer (25 mM TRIS pH 8 with or without 0.5 mM $ZnCl_2$) were mixed together and spectra were taken immediately, after 24 and 48 hours. Care was taken so the sample absorbance never exceeded 1.5 at all wavelengths to produce reliable ellipticity values.

Author Manuscript Author Manuscript Author Manuscript Author Manuscript

Ultracentrifugation studies.

Peptide and macrocycle samples were prepared immediately before experiment. The solutions contained 15 μM peptide or macrocycle, 1 mM $ZnCl_2$ in 25 mM Tris buffer (pH 8). Each sample was spun down using an ultracentrifuge (100,000 g for 1 h at 4 °C). UV-Vis spectra were acquired for the samples before ultracentrifugation and for the supernatant after ultracentrifugation using Agilent 8453 UV-Visible spectrophotometer.

Transmission electron microscopy.

Peptide stocks were diluted 10-fold to an approximate concentration of 100 μM using a buffer containing 25 mM TRIS (pH 8) and 0.1 mM $ZnCl_2$. Sample aliquots of 10 μl were adsorbed for 2–5 minutes onto formvar/carbon-coated, 200-mesh copper grids (Ted Pella). Grids were then washed briefly with water and stained with one 10 μl drop of 2% (w/v) uranyl acetate. After drying, samples were viewed with a JEOL-JEM 2100F Field Emission electron microscope at an acceleration voltage of 200 kV. Electron micrographs were recorded on a Gatan OneView 4K CCD camera.

Supplementary Material

Refer to Web version on PubMed Central for supplementary material.

Acknowledgements

This work was supported by the NIH (grant GM119634), the CRDF (grant OISE 18-63891-0), and the Alexander von Humboldt Foundation. Use of the Center for Nanoscale Materials, an Office of Science user facility, was supported by the U.S. Department of Energy, Office of Science, Office of Basic Energy Sciences, under Contract No. DE-AC02-06CH11357.

References

[1]. a)Greenwald J, Riek R, J. Mol. Biol 2012, 421, 417–426; [PubMed: 22542525] b)Maury CPJ, Cell. Mol. Life. Sci, 2018, 75, 1499–1507. [PubMed: 29550973]

[2]. a)Fleming S, Ulijn RV, Chem. Soc. Rev 2014, 43, 8150–8177; [PubMed: 25199102] b)Maeda Y, Javid N, Duncan K, Birchall L, Gibson KF, Cannon D, Kanetsuki Y, Knapp C, Tuttle T, Ulijn RV, Matsui H, J. Am. Chem. Soc 2014, 136, 15893–15896; [PubMed: 25343575] c)Zozulia O, Dolan MA, Korendovych IV, Chem. Soc. Rev 2018, 47, 3621–3639. [PubMed: 29594277]

[3]. Emsley J, White HE, O'Hara BP, Oliva G, Srinivasan N, Tickle IJ, Blundell TL, Pepys MB, Wood SP, Nature 1994, 367, 338–345. [PubMed: 8114934]

[4]. Rufo CM, Moroz YS, Moroz OV, Stöhr J, Smith TA, Hu X, DeGrado WF, Korendovych IV, Nat. Chem 2014, 6, 303–309. [PubMed: 24651196]

[5]. a)Lee M, Wang T, Makhlynets OV, Wu Y, Polizzi NF, Wu H, Gosavi PM, Stöhr J, Korendovych IV, DeGrado WF, Hong M, Proc. Natl. Acad. Sci. U. S. A 2017, 114, 6191–6196; [PubMed: 28566494] b)Song R, Wu X, Xue B, Yang Y, Huang W, Zeng G, Wang J, Li W, Cao Y, Wang W, Lu J, Dong H, J. Am. Chem. Soc 2019, 141, 223–231. [PubMed: 30562022]

[6]. Marshall LR, Zozulia O, Lengyel-Zhand Z, Korendovych IV, ACS Catal 2019, 9, 9265–9275.

[7]. a)Al-Garawi ZS, McIntosh BA, Neill-Hall D, Hatimy AA, Sweet SM, Bagley MC, Serpell LC, Nanoscale 2017, 9, 10773–10783; [PubMed: 28722055] b)Dolan MA, Basa PN, Zozulia O, Lengyel Z, Lebl R, Kohn EM, Bhattacharya S, Korendovych IV, ACS Nano 2019, 13, 9292–9297; [PubMed: 31314486] c)Zozulia O, Korendovych IV, Angew. Chem. Int. Ed 2020, 59, 8108–8112;d)Monasterio O, Nova E, Diaz-Espinoza R, Biochem. Biophys. Res. Commun 2017, 482, 1194–1200; [PubMed: 27923655] e)Lengyel Z, Rufo CM, Moroz YS, Makhlynets OV, Korendovych IV, ACS Catal 2018, 8, 59–62; [PubMed: 30319881] f)Makhlynets OV, Gosavi PM,

Author Manuscript Author Manuscript Author Manuscript Author Manuscript

Korendovych IV, Angew. Chem. Int. Ed 2016, 55, 9017–9020;g)Solomon LA, Kronenberg JB, Fry HC, J. Am. Chem. Soc 2017, 139, 8497–8507; [PubMed: 28505436] h)Pelin JNBD, Gerbelli BB, Soares BM, Aguilar AM, Alves WA, Catal. Sci. Technol, 2019, 9, 4304–4313.

[8]. Marshall LR, Jayachandran M, Lengyel-Zhand Z, Rufo CM, Kriews A, Kim M-C, Korendovych IV, ChemBioChem 2020, doi: 10.1002/cbic.202000205

[9]. a)Nanda J, Rubinov B, Ivnitski D, Mukherjee R, Shtelman E, Motro Y, Miller Y, Wagner N, Cohen-Luria R, Ashkenasy G, Nat. Comm, 2017, 8, 434;b)Tena-Solsona M, Nanda J, Díaz-Oltra S, Chotera A, Ashkenasy G, Escuder B, Chem. Eur. J, 2016, 22, 6687–6694; [PubMed: 27004623] c)Brack A, Chem. Biodivers, 2007, 4, 665–679; [PubMed: 17443882] d)Rubinov B, Wagner N, Rapaport H, Ashkenasy G, Angew. Chem. Int. Ed 2009, 48, 6683–6686;e)Rubinov B, Wagner N, Matmor M, Regev O, Ashkenasy N, Ashkenasy G, ACS Nano 2012, 6, 7893–7901; [PubMed: 22856322] f)Maury CPJ, Orig. life. Evol. Biosph, 2009, 39, 141–150. [PubMed: 19301141]

[10]. a)Smith CK, Regan L, Acc. Chem. Res 1997, 30, 153–161;b)Gellman SH, Curr. Opin. Chem. Biol 1998, 2, 717–725; [PubMed: 9914187] c)Marcos E, Chidyausiku TM, McShan AC, Evangelidis T, Nerli S, Carter L, Nivón LG, Davis A, Oberdorfer G, Tripsianes K, Sgourakis NG, Baker D, Nat. Struct. Mol. Biol 2018, 25, 1028–1034. [PubMed: 30374087]

[11]. a)Khakshoor O, Nowick JS, Curr. Opin. Chem. Biol 2008, 12, 722–729; [PubMed: 18775794] b)Cheng P-N, Pham JD, Nowick JS, J. Am. Chem. Soc 2013, 135, 5477–5492. [PubMed: 23548073]

[12]. a)Nowick JS, Chung DM, Maitra K, Maitra S, Stigers KD, Sun Y, J. Am. Chem. Soc 2000, 122, 7654–7661;b)Woods RJ, Brower JO, Castellanos E, Hashemzadeh M, Khakshoor O, Russu WA, Nowick JS, J. Am. Chem. Soc 2007, 129, 2548–2558. [PubMed: 17295482]

[13]. a)Eckhardt B, Grosse W, Essen L-O, Geyer A, Proc. Natl. Acad. Sci. U. S. A 2010, 107, 18336–18341; [PubMed: 20937907] b)Körling M, Geyer A, Eur. J. Org. Chem 2015, 2015, 6448–6457.

[14]. Klein JS, Jiang S, Galimidi RP, Keeffe JR, Bjorkman PJ, Protein Eng Des Sel 2014, 27, 325–330. [PubMed: 25301959]

[15]. Freire F, Gellman SH, J. Am. Chem. Soc 2009, 131, 7970–7972. [PubMed: 19456161]

[16]. West MW, Wang W, Patterson J, Mancias JD, Beasley JR, Hecht MH, Proc. Natl. Acad. Sci. U. S. A 1999, 96, 11211–11216. [PubMed: 10500156]

Author Manuscript Author Manuscript Author Manuscript Author Manuscript

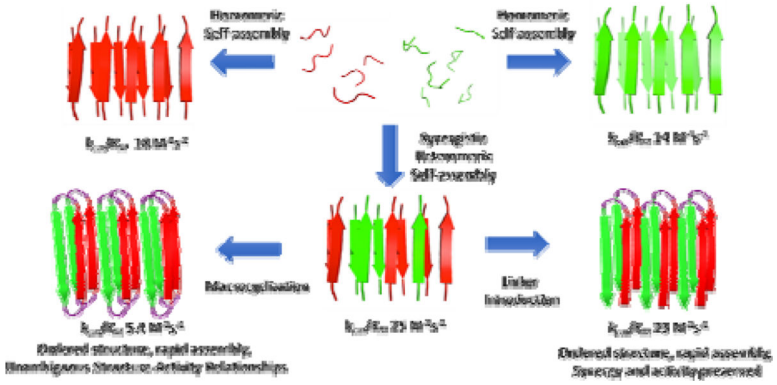

Figure 1.

Short peptides can self-assemble into homomeric catalytic amyloids capable of promoting pNPA hydrolysis. Heteromeric catalytic amyloids offer synergistic interaction to further improve catalytic activity. Introduction of linkers locks the productive arrangements of functional groups in place and promotes faster fibril formation. Zinc ions omitted for clarity of the heteromeric assembly.

Author Manuscript Author Manuscript Author Manuscript Author Manuscript

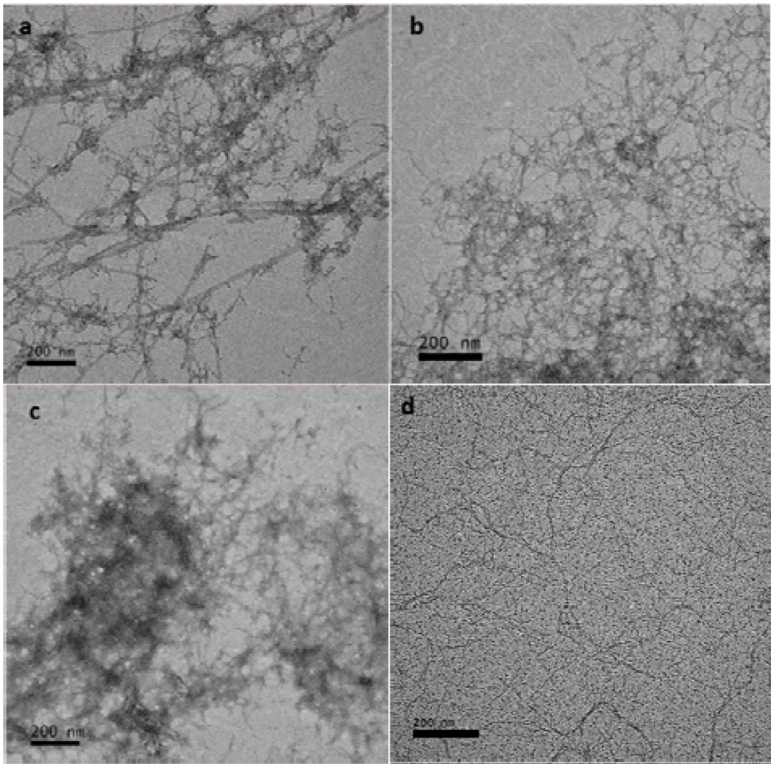

Figure 2.
TEM images of fibrils formed by a) **gggQQ** b) **oQQ** c) **htQQ** d) **t^RR**.

Author Manuscript Author Manuscript Author Manuscript Author Manuscript

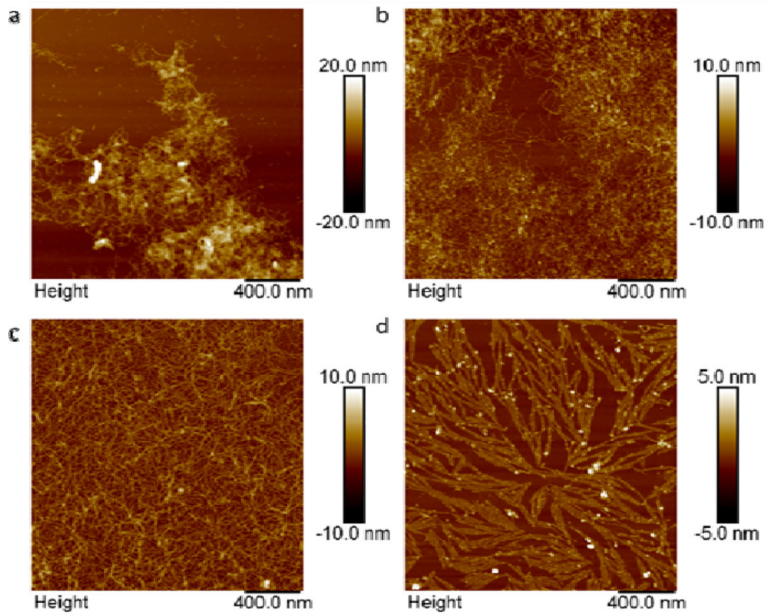

Figure 3.

AFM images of fibrils formed by a) **mQQ$_a$** b) **mYR** c) **mQQ$_p$** d) **mYY**.

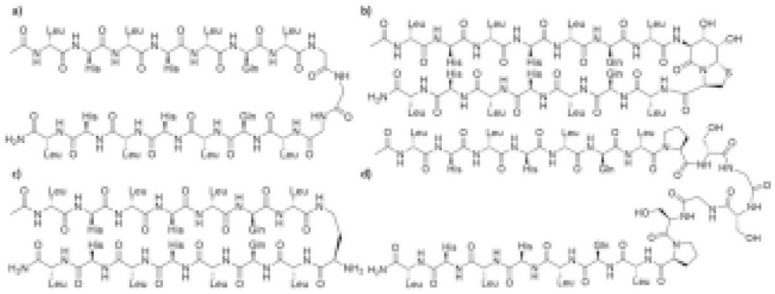

Scheme 1.

Linkers used to connect catalytic amyloid-forming peptides. a) gggQQ b) htQQ c) oQQ d) t^QQ

Author Manuscript Author Manuscript Author Manuscript Author Manuscript

Author Manuscript Author Manuscript Author Manuscript Author Manuscript

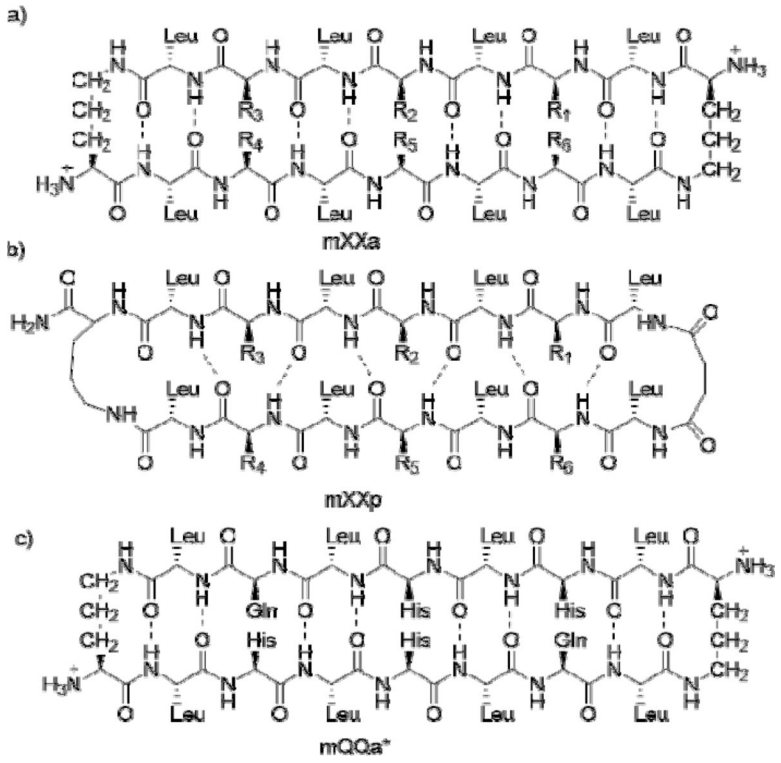

Scheme 2.

Structures of the macrocycles prepared in this study in both the a) antiparallel (mXX_a) and b) parallel (mXX_p) orientations, where X describes the active residues present in the R_3 and R_4 residues. R' and R" indicate the location of methylation in **mQQ$_m$** and **mQQ$_{mm}$**. The panel c) shows **mQQ$_{a*}$** with sidechain residues explicitly labelled.

Author Manuscript Author Manuscript Author Manuscript Author Manuscript

Table 1.

Kinetic parameters for pNPA hydrolysis for the catalytic amyloid-forming peptides. Conditions: 25 μM peptide, 0.1 mM $ZnCl_2$, 25 mM Tris buffer, pH 8.0.

Peptide	k_{cat} ($\times 10^{-2}$ s^{-1})	K_M (mM)	k_{cat}/K_M (M^{-1} s^{-1})
Ac-LHLHLQL-NH2	1.8 ± 0.38	0.54 ± 0.2	30 ± 3[a]
Ac-LHLHLRL-NH_2	3.2 ± 0.4	1.8 ± 0.4	18.4 ±4[a]
Ac-LHLHLYL-NH_2	0.7 ± 0.08	0.6 ± 0.1	13.5 ±5[a]
htQQ	n.d.	n.d.	2.0 ± 0.1
oQQ	0.35 ± 0.22	0.9 ± 0.9	3.8 ± 1.5
gggQQ	0.49 ± 0.22	1.1 ± 0.8	4.3 ± 2.7
t^QQ	2.2 ± 0.03	0.87 ± 0.11	24.9 ± 1.3
t^RR	1.54 ± 0.2	0.8 ± 0.2	19.3 ± 0.3
t^YY	0.15 ± 0.002	0.34 ± 0.07	4.5 ± 0.3
t^YR	2.49 ± 0.05	1.07 ± 0.25	23.2 ± 1.5
t^QR	2.89 ± 0.04	0.82 ± 0.02	35.5 ± 0.6
t^RQ	3.26 ± 0.15	0.92 ± 0.07	35.5 ± 1.0
t^QQ/t^RR (1:1)	2.5 ± 0.2	0.8 ± 0.1	31 ± 5.0

[a] after 24 h, taken from Rufo *et. al.*[7]

ht (Hot=Tap), o (L-ornithine), ggg (GlyGlyGly), t^ (PSGSGSP); n.d. – not determined due to the lack of initial rate saturation in the concentration range of pNPA studied.

Author Manuscript

Author Manuscript

Author Manuscript

Author Manuscript

Table 2.

Kinetic parameters for pNPA hydrolysis catalyzed by the macrocyclic amyloid-forming peptides. Experimental conditions: 15 μM peptide, 0.1 mM Zn, 25 mM Tris, pH 8.0.

	R1	R2	R3	R4	R5	R6	k_{cat}/K_M (M^{-1} s^{-1})
mQQa	H	H	Q	Q	H	H	6.3 ± 0.9
mQQp	H	H	Q	Q	H	H	5.8 ± 0.7
mQQa*	H	H	Q	H	H	Q	1.1 ± 0.5
mQQm	H	H_{Me}	Q	Q	H	H	0.96 ± 0.04
mQQmm	H	H_{Me}	Q	Q	H_{Me}	H	0.6 ± 0.1
mRRp	H	H	R	R	H	H	4.3 ± 0.4
mRRa	H	H	R	R	H	H	3.2 ± 0.8
mYYa	H	H	Y	Y	H	H	1.9 ± 0.6
mYRa	H	H	Y	Y	H	H	5.4 ± 2.0

*a=antiparallel, p=parallel, m= N-methylhistidine substitution